

# Supplementary Materials for “A Ready To Use Web-Application Providing a Personalized Biopsy Schedule for Men With Low-Risk PCa Under Active Surveillance”

Anirudh Tomer, MSc<sup>a,\*</sup>, Daan Nieboer, MSc<sup>b</sup>, Monique J. Roobol, PhD<sup>c</sup>, Anders Bjartell, MD, PhD<sup>d</sup>, Ewout W. Steyerberg, PhD<sup>b,e</sup>, Dimitris Rizopoulos, PhD<sup>a</sup>, Movember Foundations Global Action Plan Prostate Cancer Active Surveillance (GAP3) consortium<sup>f</sup>

<sup>a</sup>*Department of Biostatistics, Erasmus University Medical Center, Rotterdam, the Netherlands*

<sup>b</sup>*Department of Public Health, Erasmus University Medical Center, Rotterdam, the Netherlands*

<sup>c</sup>*Department of Urology, Erasmus University Medical Center, Rotterdam, the Netherlands*

<sup>d</sup>*Department of Urology, Skåne University Hospital, Malmö, Sweden*

<sup>e</sup>*Department of Biomedical Data Sciences, Leiden University Medical Center, Leiden, the Netherlands*

<sup>f</sup>*The Movember Foundations Global Action Plan Prostate Cancer Active Surveillance (GAP3) consortium members presented in Appendix F*

---

## 1 Appendix A. A Joint Model for the Longitudinal PSA, and Time 2 to Gleason Upgrading

3 Let  $T_i^*$  denote the true time of upgrading (increase in biopsy Gleason  
4 grade group from 1 to 2 or higher) for the  $i$ -th patient included in PRIAS.  
5 Since biopsies are conducted periodically,  $T_i^*$  is observed with interval cen-  
6 soring  $l_i < T_i^* \leq r_i$ . When upgrading is observed for the patient at his latest

---

\*Corresponding author (Anirudh Tomer): Erasmus MC, kamer flex Na-2823, PO Box 2040, 3000 CA Rotterdam, the Netherlands. Tel: +31 10 70 43393

*Email addresses:* [a.tomer@erasmusmc.nl](mailto:a.tomer@erasmusmc.nl) (Anirudh Tomer, MSc),  
[d.nieboer@erasmusmc.nl](mailto:d.nieboer@erasmusmc.nl) (Daan Nieboer, MSc), [m.roobol@erasmusmc.nl](mailto:m.roobol@erasmusmc.nl) (Monique J. Roobol, PhD), [anders.bjartell@med.lu.se](mailto:anders.bjartell@med.lu.se) (Anders Bjartell, MD, PhD),  
[e.w.steyerberg@lumc.nl](mailto:e.w.steyerberg@lumc.nl) (Ewout W. Steyerberg, PhD), [d.rizopoulos@erasmusmc.nl](mailto:d.rizopoulos@erasmusmc.nl) (Dimitris Rizopoulos, PhD)

7 biopsy time  $r_i$ , then  $l_i$  denotes the time of the second latest biopsy. Oth-  
 8 erwise,  $l_i$  denotes the time of the latest biopsy and  $r_i = \infty$ . Let  $\mathbf{y}_i$  denote  
 9 his observed PSA longitudinal measurements. The observed data of all  $n$   
 10 patients is denoted by  $\mathcal{D}_n = \{l_i, r_i, \mathbf{y}_i; i = 1, \dots, n\}$ .

In our joint model, the patient-specific PSA measurements over time are modeled using a linear mixed effects sub-model. It is given by (see Panel A, Figure 1):

$$\begin{aligned} \log_2 \{y_i(t) + 1\} &= m_i(t) + \varepsilon_i(t), \\ m_i(t) &= \beta_0 + b_{0i} + \sum_{k=1}^4 (\beta_k + b_{ki}) B_k\left(\frac{t-2}{2}, \frac{\mathcal{K}-2}{2}\right) + \beta_5 \text{age}_i, \end{aligned} \quad (1)$$

11 where,  $m_i(t)$  denotes the measurement error free value of  $\log_2(\text{PSA} + 1)$   
 12 transformed  $[2, 3]$  measurements at time  $t$ . We model it non-linearly over  
 13 time using B-splines [4]. To this end, our B-spline basis function  $B_k\{(t -$   
 14  $2)/2, (\mathcal{K} - 2)/2\}$  has 3 internal knots at  $\mathcal{K} = \{0.5, 1.3, 3\}$  years, which are  
 15 the three quartiles of the observed follow-up times. The boundary knots of  
 16 the spline are at 0 and 6.3 years (95-th percentile of the observed follow-  
 17 up times). We mean centered (mean 2 years) and standardized (standard  
 18 deviation 2 years) the follow-up time  $t$  and the knots of the B-spline  $\mathcal{K}$  during  
 19 parameter estimation for better convergence. The fixed effect parameters are  
 20 denoted by  $\{\beta_0, \dots, \beta_5\}$ , and  $\{b_{0i}, \dots, b_{4i}\}$  are the patient specific random  
 21 effects. The random effects follow a multivariate normal distribution with  
 22 mean zero and variance-covariance matrix  $\mathbf{D}$ . The error  $\varepsilon_i(t)$  is assumed to  
 23 be t-distributed with three degrees of freedom (see Appendix B.1) and scale  
 24  $\sigma$ , and is independent of the random effects.

To model the impact of PSA measurements on the risk of upgrading, our joint model uses a relative risk sub-model. More specifically, the hazard of upgrading denoted as  $h_i(t)$ , and the cumulative-risk of upgrading denoted as  $R_i(t)$ , at a time  $t$  are (see Panel C, Figure 1):

$$\begin{aligned} h_i(t) &= h_0(t) \exp\left(\gamma \text{age}_i + \alpha_1 m_i(t) + \alpha_2 \frac{dm_i(t)}{dt}\right), \\ R_i(t) &= \exp\left\{-\int_0^t h_i(s) ds\right\}, \end{aligned} \quad (2)$$

where,  $\gamma$  is the parameter for the effect of age. The impact of PSA on the hazard of upgrading is modeled in two ways, namely the impact of the error

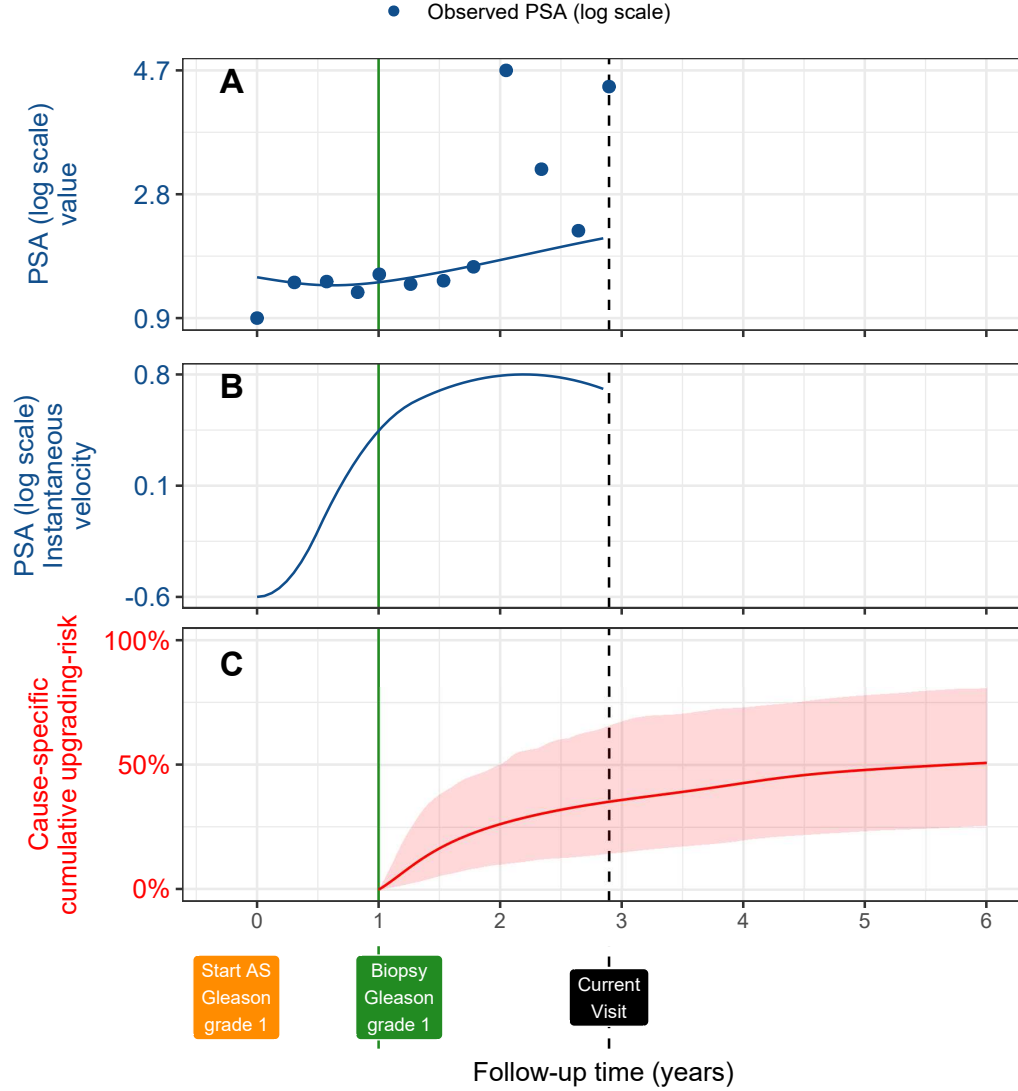


Figure 1: **Illustration of the joint model on a real PRIAS dataset patient.** **Panel A:** Observed (blue dots) and fitted PSA (solid blue line) measurements, log-transformed. **Panel B:** Estimated instantaneous velocity of PSA (log-transformed). **Panel C:** Predicted cumulative-risk of upgrading (95% credible interval shaded). Upgrading is defined as increase in Gleason grade group [1] from grade group 1 to 2 or higher. This risk of upgrading is available starting from the time of the latest negative biopsy (vertical green line at year 1 of follow-up). Joint model estimated it by combining the fitted PSA value and velocity (both on log scale of PSA) and time of latest negative biopsy. Black dashed line at year 4 denotes time of current visit.

free underlying PSA value  $m_i(t)$  (see Panel A, Figure 1), and the impact of the underlying PSA velocity  $dm_i(t)/dt$  (see Panel B, Figure 1). The corresponding parameters are  $\alpha_1$  and  $\alpha_2$ , respectively. Lastly,  $h_0(t)$  is the baseline hazard at time  $t$ , and is modeled flexibly using P-splines [5]. More specifically:

$$\log h_0(t) = \gamma_{h_0,0} + \sum_{q=1}^Q \gamma_{h_0,q} B_q(t, \mathbf{v}),$$

25 where  $B_q(t, \mathbf{v})$  denotes the  $q$ -th basis function of a B-spline with knots  $\mathbf{v} =$   
 26  $v_1, \dots, v_Q$  and vector of spline coefficients  $\gamma_{h_0}$ . To avoid choosing the number  
 27 and position of knots in the spline, a relatively high number of knots (e.g.,  
 28 15 to 20) are chosen and the corresponding B-spline regression coefficients  
 29  $\gamma_{h_0}$  are penalized using a differences penalty [5].

We estimate the parameters of the joint model using Markov chain Monte Carlo (MCMC) methods under the Bayesian framework. Let  $\boldsymbol{\theta}$  denote the vector of all of the parameters of the joint model. The joint model postulates that given the random effects, the time of upgrading, and the PSA measurements taken over time are all mutually independent. Under this assumption the posterior distribution of the parameters is given by:

$$\begin{aligned} p(\boldsymbol{\theta}, \mathbf{b} \mid \mathcal{D}_n) &\propto \prod_{i=1}^n p(l_i, r_i, \mathbf{y}_i \mid \mathbf{b}_i, \boldsymbol{\theta}) p(\mathbf{b}_i \mid \boldsymbol{\theta}) p(\boldsymbol{\theta}) \\ &\propto \prod_{i=1}^n p(l_i, r_i \mid \mathbf{b}_i, \boldsymbol{\theta}) p(\mathbf{y}_i \mid \mathbf{b}_i, \boldsymbol{\theta}) p(\mathbf{b}_i \mid \boldsymbol{\theta}) p(\boldsymbol{\theta}), \\ p(\mathbf{b}_i \mid \boldsymbol{\theta}) &= \frac{1}{\sqrt{(2\pi)^q \det(\mathbf{D})}} \exp \left\{ -\frac{1}{2} (\mathbf{b}_i^T \mathbf{D}^{-1} \mathbf{b}_i) \right\}, \end{aligned}$$

where, the likelihood contribution of the PSA outcome, conditional on the random effects is:

$$p(\mathbf{y}_i \mid \mathbf{b}_i, \boldsymbol{\theta}) = \frac{1}{(\sqrt{2\pi}\sigma^2)^{n_i}} \exp \left\{ -\frac{\sum_{j=1}^{n_i} (y_{ij} - m_{ij})^2}{2\sigma^2} \right\},$$

where  $n_i$  is the number of PSA measurements of the  $i$ -th patient. The likelihood contribution of the time of upgrading outcome is given by:

$$p(l_i, r_i \mid \mathbf{b}_i, \boldsymbol{\theta}) = \exp \left\{ -\int_0^{l_i} h_i(s) ds \right\} - \exp \left\{ -\int_0^{r_i} h_i(s) ds \right\}. \quad (3)$$

30 The integrals in (3) do not have a closed-form solution, and therefore we use  
 31 a 15-point Gauss-Kronrod quadrature rule to approximate them.

32 We use independent normal priors with zero mean and variance 100 for  
 33 the fixed effects  $\{\beta_0, \dots, \beta_5\}$ , and inverse Gamma prior with shape and rate  
 34 both equal to 0.01 for the parameter  $\sigma^2$ . For the variance-covariance matrix  
 35  $\mathbf{D}$  of the random effects we take inverse Wishart prior with an identity scale  
 36 matrix and degrees of freedom equal to 5 (number of random effects). For  
 37 the relative risk model's parameter  $\gamma$  and the association parameters  $\alpha_1, \alpha_2$ ,  
 38 we use independent normal priors with zero mean and variance 100.

### 39 *Appendix A.1. Assumption of t-distributed (df=3) Error Terms*

40 With regards to the choice of the distribution for the error term  $\varepsilon$  for  
 41 the PSA measurements (see Equation 1), we attempted fitting multiple joint  
 42 models differing in error distribution, namely t-distribution with three, and  
 43 four degrees of freedom, and a normal distribution for the error term. How-  
 44 ever, the model assumption for the error term were best met by the model  
 45 with t-distribution having three degrees of freedom. The quantile-quantile  
 46 plot of subject-specific residuals for the corresponding model in Panel A of  
 47 Figure 2, shows that the assumption of t-distributed (df=3) errors is reason-  
 48 ably met by the fitted model.

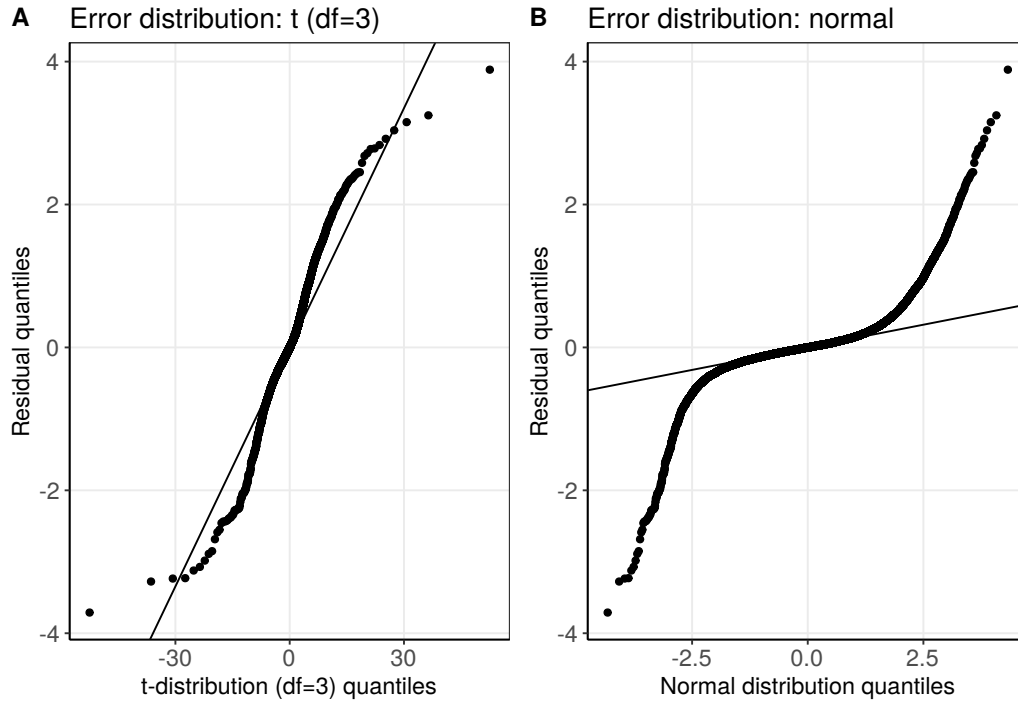


Figure 2: **Quantile-quantile plot** of subject-specific PSA residuals from two different joint models fitted to the PRIAS dataset. **Panel A:** model assuming a t-distribution ( $df=3$ ) for the error term  $\varepsilon$  (see Equation 1). **Panel B:** model assuming a normal distribution for the error term  $\varepsilon$ . We selected the model with t-distributed error terms.

49 *Appendix A.2. Results*

50 Characteristics of the five validation cohorts from the GAP3 database [6]  
 51 are shown in Table 1. The cause-specific cumulative upgrading-risk in these  
 52 cohorts is shown in Figure 3.

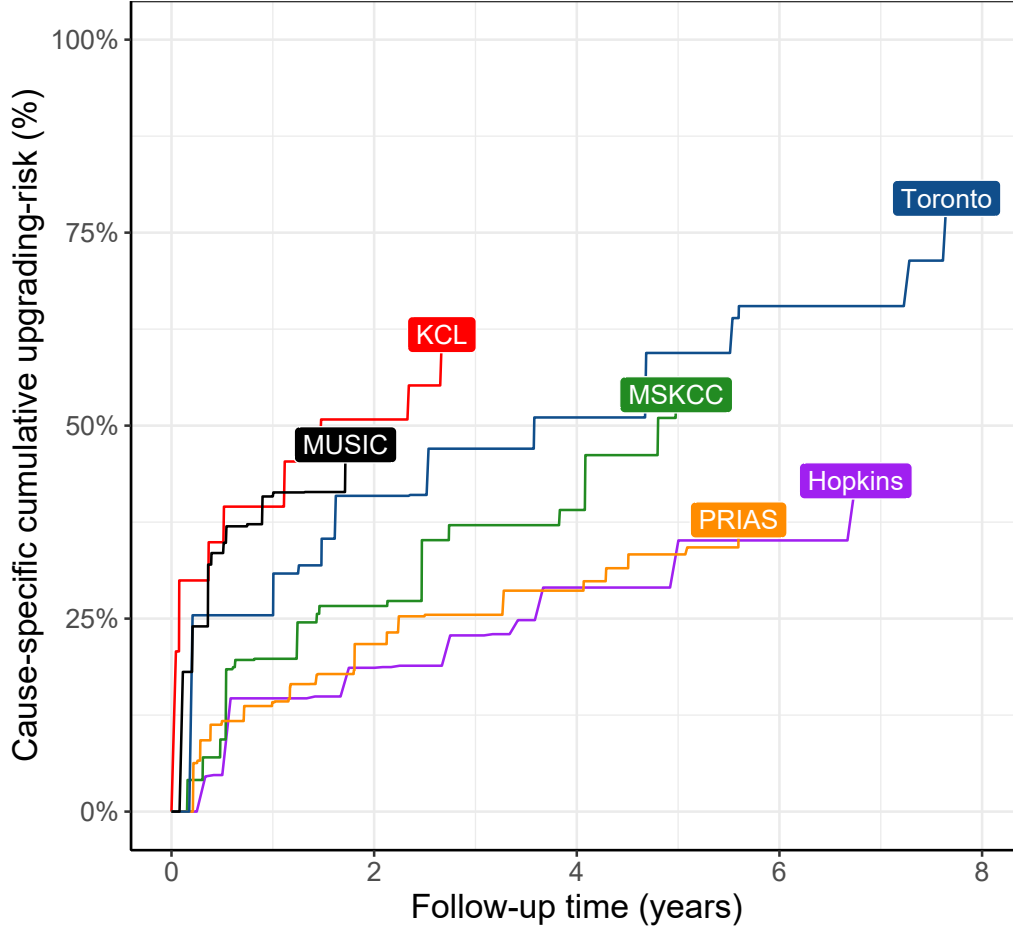


Figure 3: **Nonparametric estimate [7] of the cause-specific cumulative upgrading-risk** in the world's largest AS cohort PRIAS, and largest five AS cohorts from the GAP3 database [6]. Abbreviations are *Hopkins*: Johns Hopkins Active Surveillance, *PRIAS*: Prostate Cancer International Active Surveillance, *Toronto*: University of Toronto Active Surveillance, *MSKCC*: Memorial Sloan Kettering Cancer Center Active Surveillance, *KCL*: King's College London Active Surveillance, *MUSIC*: Michigan Urological Surgery Improvement Collaborative AS.

Table 1: **Summary of the five validation cohorts from the GAP3 database [6].** The primary event of interest is upgrading, that is, increase in Gleason grade group from group 1 to 2 or higher. #PSA: number of PSA, #biopsies: number of biopsies, IQR: interquartile range, PSA: prostate-specific antigen. Full names of cohorts are *Hopkins*: Johns Hopkins Active Surveillance, *PRIAS*: Prostate Cancer International Active Surveillance, *Toronto*: University of Toronto Active Surveillance, *MSKCC*: Memorial Sloan Kettering Cancer Center Active Surveillance, *KCL*: King's College London Active Surveillance, *MUSIC*: Michigan Urological Surgery Improvement Collaborative AS.

Characteristic	Hopkins	Toronto	MSKCC	MUSIC	KCL
Total patients	1392	1046	894	2743	616
Upgrading (primary event)	260	359	242	385	198
Median age (years)	62 (IQR: 66–69)	67 (IQR: 60–72)	63 (IQR: 57–68)	65 (IQR: 60–71)	63 (IQR: 58–68)
Median follow-up per patient (years)	3 (IQR: 1.3–5.8)	4.5 (IQR: 1.9–8.4)	5.3 (IQR: 1.8–8.3)	1.2 (IQR: 0.6–2.2)	2.4 (IQR: 1.3–3.8)
Total PSA measurements	11126	13984	10704	12087	2987
Median #PSA per patient	6 (IQR: 4–11)	12 (IQR: 7–19)	11 (IQR: 5–17)	4 (IQR: 2–6)	4 (IQR: 2–6)
Median PSA (ng/mL)	4.7 (IQR: 2.9–6.7)	6 (IQR: 3.7–9.0)	4.7 (IQR: 2.8–7.1)	5.1 (IQR: 3.4–7.1)	6 (IQR: 4–9)
Total biopsies	1926	909	1102	1032	484
Median #biopsies per patient	1 (IQR: 1–2)	1 (IQR: 1–2)	1 (IQR: 1–2)	1 (IQR: 1–1)	1 (IQR: 1–1)



Table 2: **Estimated variance-covariance matrix  $\mathbf{D}$**  of the random effects  $\mathbf{b} = (b_0, b_1, b_2, b_3, b_4)$  from the joint model fitted to the PRIAS dataset. The variances of the random effects are highlighted along the diagonal of the variance-covariance matrix.

Random Effects	$b_0$	$b_1$	$b_2$	$b_3$	$b_4$
$b_0$	<b>0.229</b>	0.030	0.023	0.073	0.007
$b_1$	0.030	<b>0.149</b>	0.098	0.171	0.085
$b_2$	0.023	0.098	<b>0.276</b>	0.335	0.236
$b_3$	0.073	0.171	0.335	<b>0.560</b>	0.359
$b_4$	0.007	0.085	0.236	0.359	<b>0.351</b>

The joint model was fitted using the R package **JMbayes** [8]. This package utilizes the Bayesian methodology to estimate model parameters. The corresponding posterior parameter estimates are shown in Table 3 (longitudinal sub-model for PSA outcome) and Table 4 (relative risk sub-model). The parameter estimates for the variance-covariance matrix  $\mathbf{D}$  from the longitudinal sub-model for PSA are shown in the following Table 2:

For the PSA mixed effects sub-model parameter estimates (see Equation 1), in Table 3 we can see that the age of the patient trivially affects the baseline  $\log_2(\text{PSA} + 1)$  measurement. Since the longitudinal evolution of  $\log_2(\text{PSA} + 1)$  measurements is modeled with non-linear terms, the interpretation of the coefficients corresponding to time is not straightforward. In lieu of the interpretation, in Figure 4 we present plots of observed versus fitted PSA profiles for nine randomly selected patients.

For the relative risk sub-model (see Equation 2), the parameter estimates in Table 4 show that  $\log_2(\text{PSA} + 1)$  velocity and age of the patient were significantly associated with the hazard of upgrading.

It is important to note that since age, and  $\log_2(\text{PSA} + 1)$  value and velocity are all measured on different scales, a comparison between the corresponding parameter estimates is not easy. To this end, in Table 5, we present the hazard ratio of upgrading, for an increase in the aforementioned variables from their 25-th to the 75-th percentile. For example, an increase in fitted  $\log_2(\text{PSA} + 1)$  velocity from -0.085 to 0.308 (fitted 25-th and 75-th percentiles) corresponds to a hazard ratio of 2.433. The interpretation for the rest is similar.

Table 3: **Parameters of the longitudinal sub-model:** Estimated mean and 95% credible interval for parameters in Equation (1).

Variable	Mean	Std. Dev	2.5%	97.5%	P
Intercept	2.129	0.060	2.009	2.244	<0.001
Age	0.008	0.001	0.007	0.010	<0.001
Spline: [0.0, 0.5] years	0.063	0.007	0.051	0.075	<0.001
Spline: [0.5, 1.3] years	0.196	0.010	0.177	0.217	<0.001
Spline: [1.3, 3.0] years	0.244	0.014	0.217	0.272	<0.001
Spline: [3.0, 6.3] years	0.382	0.014	0.356	0.410	<0.001
$\sigma$	0.139	0.001	0.138	0.140	

Table 4: **Parameters of the relative risk sub-model:** Estimated mean and 95% credible interval for the parameters in Equation (2).

Variable	Mean	Std. Dev	2.5%	97.5%	P
Age	0.037	0.006	0.025	0.049	<0.001
Fitted $\log_2(\text{PSA} + 1)$ value	-0.012	0.076	-0.164	0.135	0.856
Fitted $\log_2(\text{PSA} + 1)$ velocity	2.266	0.299	1.613	2.767	<0.001

Table 5: **Hazard ratio and 95% credible interval (CI) for upgrading:** Variables are on different scale and hence we compare an increase in the variables of relative risk sub-model from their 25-th percentile ( $P_{25}$ ) to their 75-th percentile ( $P_{75}$ ). Except for age, quartiles for all other variables are based on their fitted values obtained from the joint model fitted to the PRIAS dataset.

Variable	$P_{25}$	$P_{75}$	Hazard ratio [95% CI]
Age	61	71	1.455 [1.285, 1.631]
Fitted $\log_2(\text{PSA} + 1)$ value	2.360	3.078	0.991 [0.889, 1.102]
Fitted $\log_2(\text{PSA} + 1)$ velocity	-0.085	0.308	2.433 [1.883, 2.962]

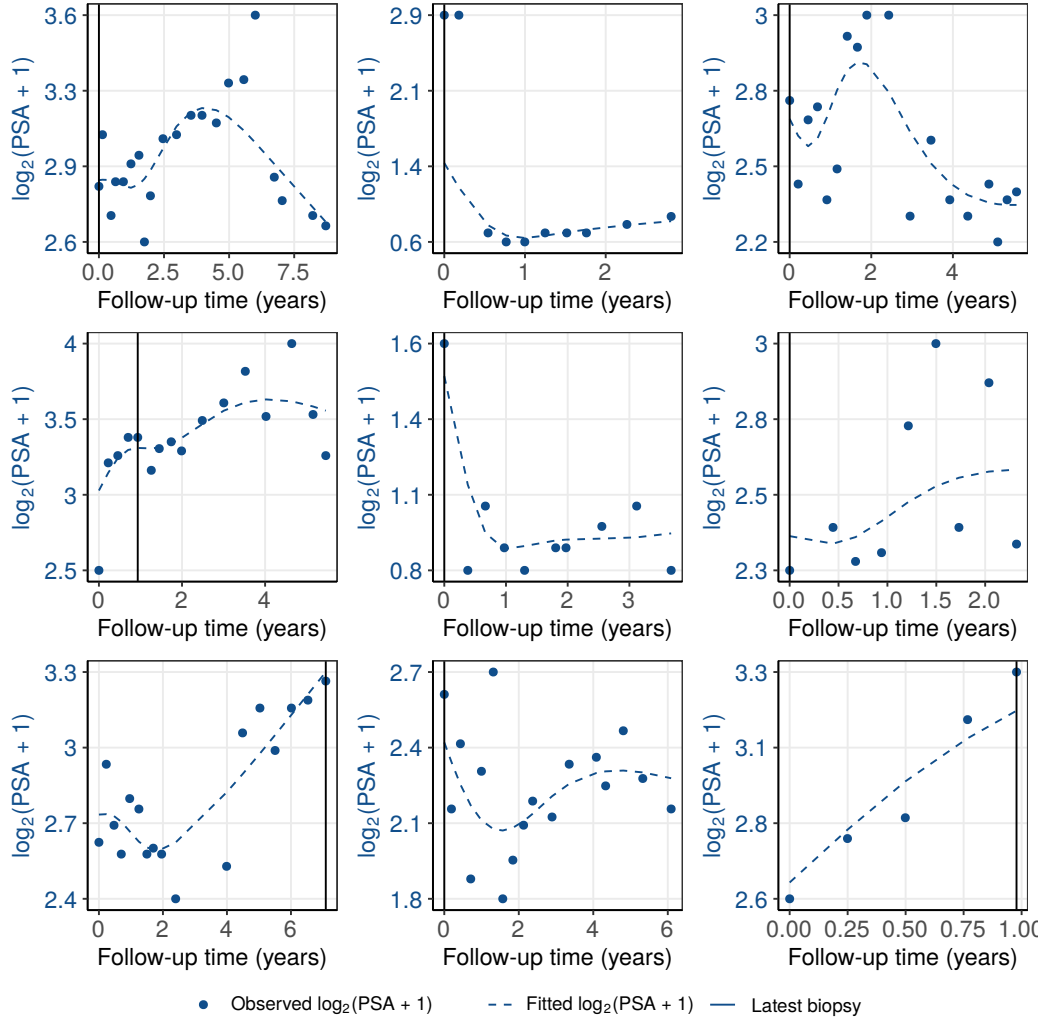


Figure 4: **Fitted versus observed  $\log_2(\text{PSA} + 1)$  profiles** for nine randomly selected PRIAS patients. The fitted profiles utilize information from the observed PSA measurements, and time of the latest biopsy.

Table 6: **Parameters of the relative risk sub-model in validation cohorts.** We fitted separate joint models for each of the five GAP3 validation cohorts as well. The specification of these joint models was same as that of the model for PRIAS. Two important predictors in the relative-risk sub-model, namely, the  $\log_2(\text{PSA} + 1)$  value and velocity have different impact on upgrading-risk across the cohorts. Table shows the mean estimate of these parameters with 95% credible interval in brackets. Strongest average effect of  $\log_2(\text{PSA} + 1)$  velocity is in PRIAS cohort, whereas the weakest is in KCL cohort. The strongest average effect of  $\log_2(\text{PSA} + 1)$  value is in the Toronto cohort whereas the weakest is in PRIAS cohort.

Cohort	Fitted $\log_2(\text{PSA} + 1)$ value	Fitted $\log_2(\text{PSA} + 1)$ velocity
PRIAS	-0.012 [-0.164, 0.135]	2.266 [ 1.613, 2.767]
Hopkins	0.061 [-0.323, 0.329]	1.839 [ 0.761, 4.378]
MSKCC	0.336 [ 0.081, 0.583]	1.122 [ 0.421, 1.980]
Toronto	0.572 [ 0.347, 0.794]	0.943 [ 0.464, 1.554]
MUSIC	0.441 [ 0.092, 0.767]	0.029 [-0.552, 0.512]
KCL	0.194 [-0.104, 0.540]	0.840 [-0.087, 1.665]

## 77 Appendix B. Risk Predictions for Upgrading

Let us assume a new patient  $j$ , for whom we need to estimate the upgrading-risk. Let his current follow-up visit time be  $s$ , latest time of biopsy be  $t$ , observed vector PSA measurements be  $\mathcal{Y}_j(s)$ . The combined information from the observed data about the time of upgrading, is given by the following posterior predictive distribution  $g(T_j^*)$  of his time  $T_j^*$  of upgrading:

$$\begin{aligned} g(T_j^*) &= p\{T_j^* \mid T_j^* > t, \mathcal{Y}_j(s), \mathcal{D}_n\} \\ &= \int \int p(T_j^* \mid T_j^* > t, \mathbf{b}_j, \boldsymbol{\theta}) \\ &\quad \times p\{\mathbf{b}_j \mid T_j^* > t, \mathcal{Y}_j(s), \boldsymbol{\theta}\} p(\boldsymbol{\theta} \mid \mathcal{D}_n) d\mathbf{b}_j d\boldsymbol{\theta}. \end{aligned}$$

78 The distribution  $g(T_j^*)$  depends not only depends on the observed data of the  
 79 patient  $T_j^* > t, \mathcal{Y}_j(s)$ , but also depends on the information from the PRIAS  
 80 dataset  $\mathcal{D}_n$ . To this the the posterior distribution of random effects  $\mathbf{b}_j$  and  
 81 posterior distribution of the vector of all parameters  $\boldsymbol{\theta}$  are utilized, respec-  
 82 tively. The distribution  $g(T_j^*)$  can be estimated as detailed in Rizopoulos  
 83 et al. [9]. Since, majority of the prostate cancer patients may not obtain  
 84 upgrading in the current follow-up period of PRIAS (thirteen years),  $g(T_j^*)$   
 85 can only be estimated for a currently limited follow-up period.

The cause-specific cumulative upgrading-risk can be derived from  $g(T_j^*)$  as given in [9]. It is given by:

$$R_j(u \mid t, s) = \Pr\{T_j^* > u \mid T_j^* > t, \mathcal{Y}_j(s), \mathcal{D}_n\}, \quad u \geq t. \quad (4)$$

86 The personalized risk profile of the patient (see Panel C, Figure 5) updates  
 87 as more data is gathered over follow-up visits.

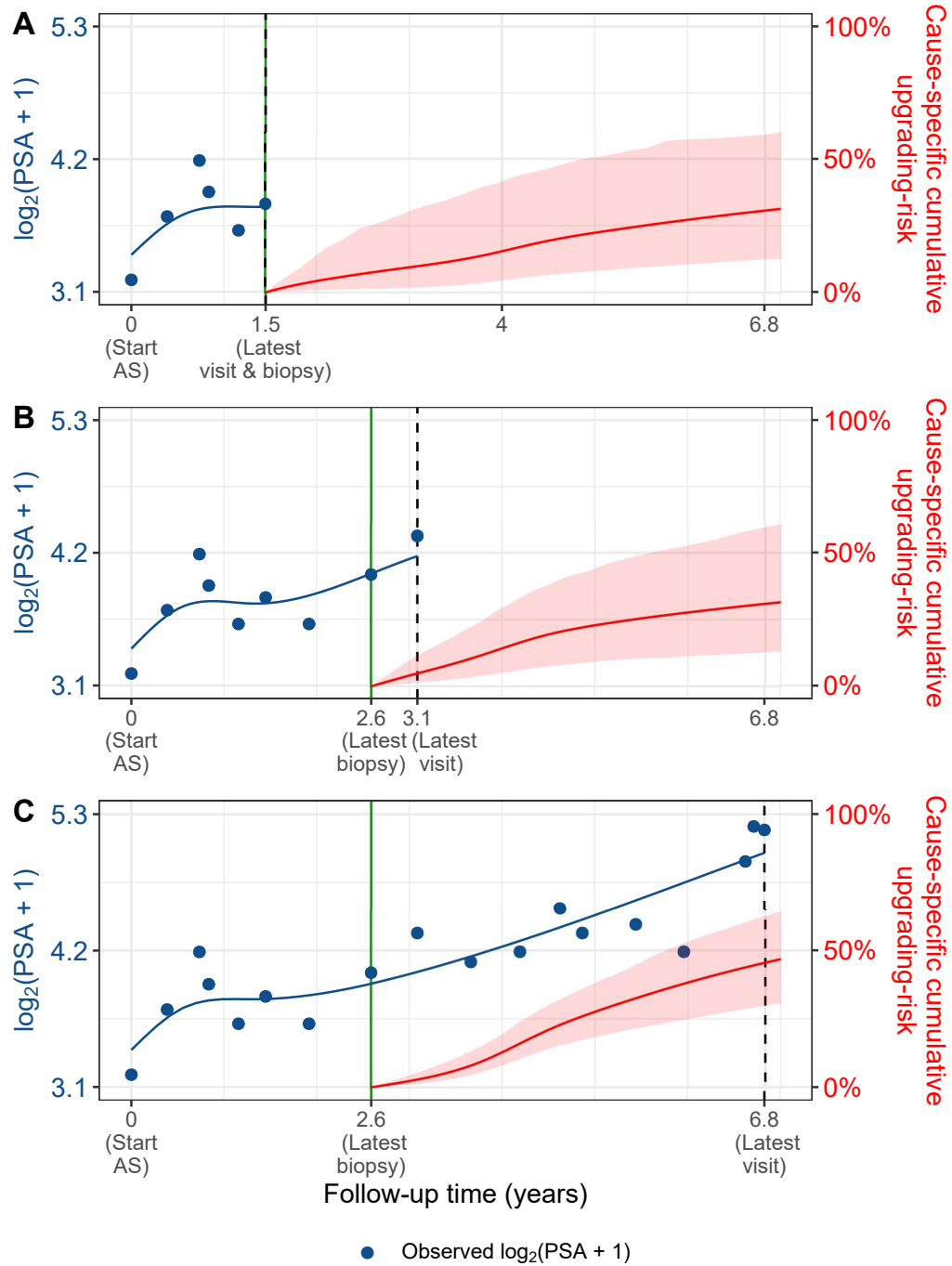


Figure 5: **Cause-specific cumulative upgrading-risk changing dynamically over follow-up** as more patient data is gathered. The three **Panels A,B and C**: are ordered by the time of the latest visit (dashed vertical black line) of a new patient. At each of the latest follow-up visits, we combine the accumulated PSA measurements (shown in blue), and latest time of negative biopsy (solid vertical green line) to obtain the updated cumulative-risk profile (shown in red) of the patient.

### 88 *Appendix B.1. Validation of Risk Predictions*

89 We wanted to check the usefulness of our model for not only the PRIAS  
 90 patients but also for patients from other cohorts. To this end, we validated  
 91 our model in the PRIAS dataset (internal validation) and in largest five co-  
 92 horts from the GAP3 database [6]. These are the University of Toronto AS  
 93 (Toronto), Johns Hopkins AS (Hopkins), Memorial Sloan Kettering Cancer  
 94 Center AS (MSKCC), King’s College London AS (KCL), and Michigan Uro-  
 95 logical Surgery Improvement Collaborative AS (MUSIC).

**Calibration-in-the-large** We first assessed calibration-in-the-large [10]  
 of our model in the aforementioned cohorts. To this end, we used our model  
 to predict the cause-specific cumulative upgrading-risk for each patient given  
 their PSA measurements and biopsy results. We then averaged the resulting  
 profiles of cause-specific cumulative upgrading-risk. Subsequently we com-  
 pared the averaged cumulative-risk profile with a non-parametric estimate [7]  
 of the cause-specific cumulative upgrading-risk in each of the cohorts. The  
 results are shown in Panel A of Figure 6. We can see that our model’s cali-  
 bration is fine only in PRIAS and Hopkins cohorts. To improve our model’s  
 calibration in KCL, MUSIC, Toronto, and MSKCC cohorts, we recalibrated  
 the baseline hazard of the joint model fitted to the PRIAS dataset, indi-  
 vidually for each of these cohorts. More specifically, given the data of an  
 external cohort  $\mathcal{D}_n^c$ , where  $c$  denotes the cohort, the recalibrated parameters  
 $\gamma_{h0}^c$  (Appendix A) of the log baseline hazard are given by:

$$p(\gamma_{h0}^c \mid \mathcal{D}_n^c, \mathbf{b}^c, \boldsymbol{\theta}) \propto \prod_{i=1}^{n^c} p(l_i^c, r_i^c \mid \mathbf{b}_i^c, \boldsymbol{\theta}) p(\gamma_{h0}^c) \quad (5)$$

96 where  $n^c$  are the number of patients in the  $c$ -th cohort and  $\boldsymbol{\theta}$  are the pa-  
 97 rameters of the joint model fitted to the PRIAS dataset. The interval in  
 98 which upgrading is observed for the  $i$  – th patient is given by  $l_i^c, r_i^c$ , with  
 99  $r_i^c = \infty$  for right censored patients. The symbol  $\mathbf{b}_i^c$  denotes patient-specific  
 100 random effects (Appendix A). The random effects are obtained using the joint  
 101 model fitted to the PRIAS dataset prior to recalibration. We re-evaluated the  
 102 calibration-in-the-large of our model after the recalibration of the baseline  
 103 hazard individually for each cohort. The improved calibration-in-the-large is  
 104 shown in Panel B of Figure 6.

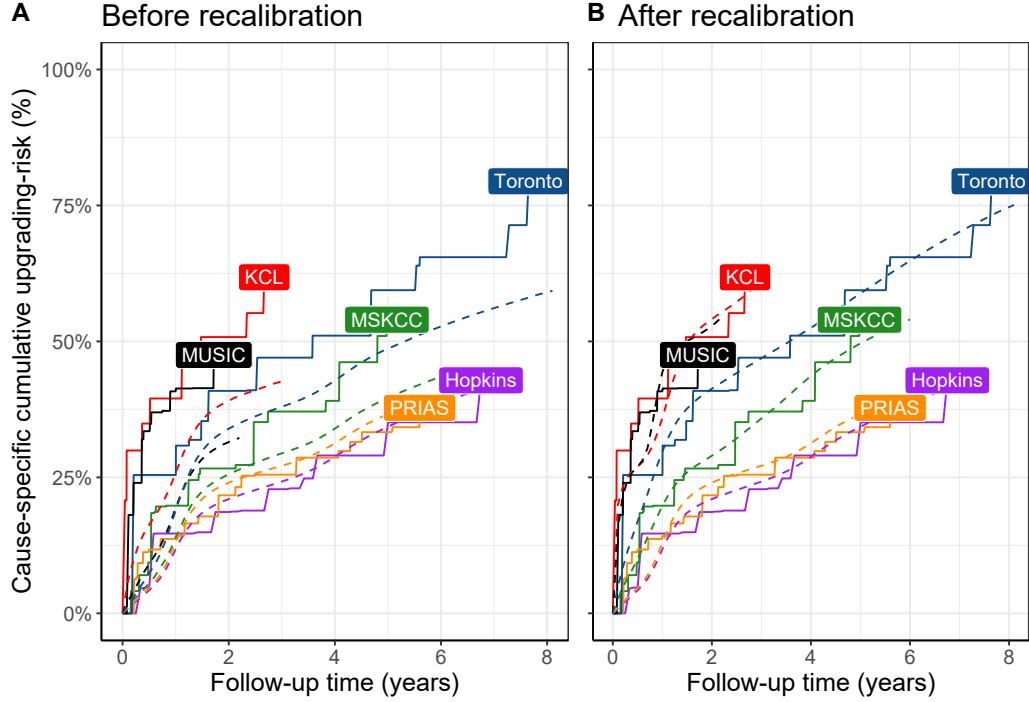


Figure 6: **Calibration-in-the-large of our model:** In **Panel A** we can see that our model is not well calibrated for use in KCL, MUSIC, Toronto and MSKCC. In **Panel B** we can see that calibration of model predictions improved in KCL, MUSIC, Toronto and MSKCC cohorts after recalibrating our model. Recalibration was not necessary for Hopkins cohort. Full names of Cohorts are *PRIAS*: Prostate Cancer International Active Surveillance, *Toronto*: University of Toronto Active Surveillance, *Hopkins*: Johns Hopkins Active Surveillance, *MSKCC*: Memorial Sloan Kettering Cancer Center Active Surveillance, *KCL*: King's College London Active Surveillance, *MUSIC*: Michigan Urological Surgery Improvement Collaborative Active Surveillance.



105 **Recalibrated PRIAS Model Versus Individual Joint Models**  
 106 **For Each Cohort** We wanted to check if our recalibrated PRIAS model  
 107 performed as good as a new joint model that could be fitted to the external  
 108 cohorts. To this end, we predicted cause-specific cumulative upgrading-risk  
 109 for each patient from each cohort using two sets of models, namely the recal-  
 110 ibrated PRIAS model for each cohort, and a new joint model fitted to each  
 111 cohort. The difference in predicted cause-specific cumulative upgrading-risk  
 112 from these models is shown in Figure 7. We can see that the difference is  
 113 smaller in those cohorts in which the effects of  $\log_2(\text{PSA} + 1)$  value and ve-  
 114 locity were similar to that of PRIAS (Table 6). For example, the Hopkins  
 115 cohort had parameter estimates similar to that of PRIAS and consequently  
 116 the difference in predicted risks for this cohort is smallest. The opposite of  
 117 this phenomenon holds true for the MUSIC and KCL cohorts.

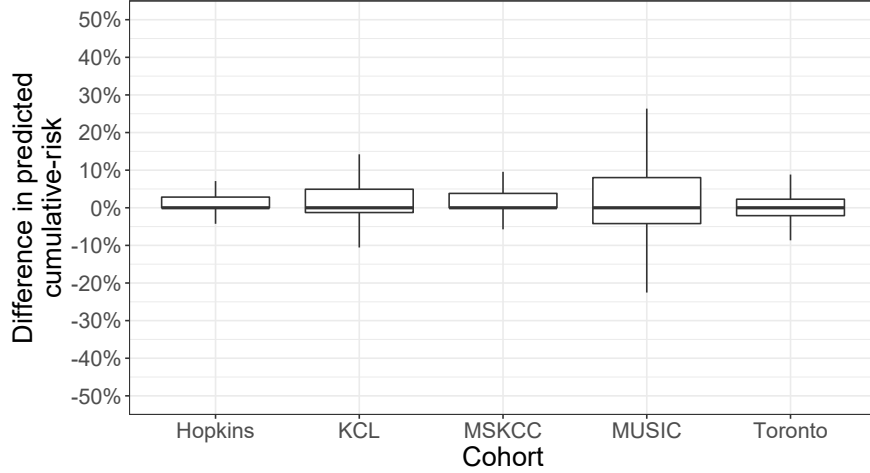


Figure 7: **Comparison of predictions from recalibrated PRIAS model with individual joint models fitted to external cohorts:** On Y-axis we show the difference between predicted cause-specific cumulative upgrading-risk for individual patients using two models, namely the recalibrated PRIAS model for each cohort, and individual joint model fitted to each cohort. The figure shows that the difference is smaller in those cohorts in which the effects of  $\log_2(\text{PSA} + 1)$  value and velocity were similar to that of PRIAS (Table 6). Full names of Cohorts are *PRIAS*: Prostate Cancer International Active Surveillance, *Toronto*: University of Toronto Active Surveillance, *Hopkins*: Johns Hopkins Active Surveillance, *MSKCC*: Memorial Sloan Kettering Cancer Center Active Surveillance, *KCL*: King’s College London Active Surveillance, *MUSIC*: Michigan Urological Surgery Improvement Collaborative Active Surveillance.

**Validation of Dynamic Cumulative-Risk Predictions** As shown in Figure 5 the cumulative-risk predictions from the joint model are dynamic in nature. That is, they update as more data becomes available over time. Consequently, the discrimination and calibration of the joint model also depends on the available data. We assessed these two measures dynamically in the PRIAS cohort (interval validation) and in the largest five external cohorts that are part of the GAP3 database. For discrimination we utilized the time-varying area under the receiver operating characteristic curve or time-varying AUC [9]. For time-varying calibration we assessed the mean absolute prediction error or MAPE [9]. The AUC indicates how well the model discriminates between patients who experience upgrading and those do not. The MAPE indicates how accurately the model predicts upgrading. Both AUC and MAPE are restricted to  $[0, 1]$ . However, it is preferred that  $\text{AUC} > 0.5$  because an  $\text{AUC} \leq 0.5$  indicates that the model performs worse than random discrimination. Ideally MAPE should be 0.

We calculate AUC and MAPE in a time-dependent manner. More specifically, given the time of latest biopsy  $t$ , and history of PSA measurements up to time  $s$ , we calculate AUC and MAPE for a medically relevant time frame  $(t, s]$ , within which the occurrence of upgrading is of interest. In the case of prostate cancer, at any point in time  $s$  it is of interest to identify patients who may have experienced upgrading in the last one year  $(s - 1, s]$ . That is we set  $t = s - 1$ . We then calculate AUC and MAPE at a gap of every six months (follow-up schedule of PRIAS). That is,  $s \in \{1, 1.5, \dots\}$  years. To obtain reliable estimates of AUC and MAPE, in each cohort we restrict  $s$  to a maximum time point  $s_{\max}$ , such that there are at least 10 patients who experience upgrading after  $s_{\max}$ . This maximum time point  $s_{\max}$  differs between cohorts, and is given in Table 7.

The results for estimates of AUC and MAPE are summarized in Figure 8, and in Table 8 to Table 13. Results are based on the recalibrated PRIAS model for the GAP3 cohorts. The results show that AUC remains more or less constant in all cohorts as more data becomes available for patients. The AUC obtains a moderate value, roughly between 0.5 and 0.7 for all cohorts. On the other hand, MAPE reduces by a big margin after year two of follow-up. This could be because of two reasons. Firstly, MAPE at year one is based only on four PSA measurements gathered in first year of follow-up, whereas after year two number of PSA measurements increase. Secondly, patients in year one consist of two sub-populations, namely patients with a correct Gleason grade group 1 at the time of inclusion in AS, and patients

Table 7: **Maximum follow-up period up to which we can reliably predict upgrading-risk.** In each cohort, this time point is chosen such that there are at least 10 patients who experience upgrading after this time point. Full names of Cohorts are *PRIAS*: Prostate Cancer International Active Surveillance, *Toronto*: University of Toronto Active Surveillance, *Hopkins*: Johns Hopkins Active Surveillance, *MSKCC*: Memorial Sloan Kettering Cancer Center Active Surveillance, *KCL*: King's College London Active Surveillance, *MUSIC*: Michigan Urological Surgery Improvement Collaborative Active Surveillance.

Cohort	Maximum Prediction Time (years)
PRIAS	6
KCL	3
MUSIC	2
Toronto	8
MSKCC	6
Hopkins	7

156 who probably had Gleason grade group 2 at inclusion but were misclassified  
 157 by the urologist as Gleason grade group 1 patients. To remedy this problem,  
 158 a biopsy for all patients at year one is commonly recommended in all AS  
 159 programs [11].

Table 8: **Internal validation of predictions of upgrading in PRIAS cohort.** The area under the receiver operating characteristic curve or AUC (measure of discrimination) and mean absolute prediction error or MAPE (measure of calibration) are calculated over the follow-up period at a gap of 6 months. In addition bootstrapped 95% confidence intervals (CI) are also presented.

Follow-up period (years)	AUC (95% CI)	MAPE (95%CI)
0.0 to 1.0	0.652 [0.611, 0.690]	0.220 [0.214, 0.227]
0.5 to 1.5	0.657 [0.641, 0.673]	0.260 [0.254, 0.265]
1.0 to 2.0	0.661 [0.647, 0.678]	0.187 [0.183, 0.191]
1.5 to 2.5	0.647 [0.596, 0.688]	0.129 [0.122, 0.140]
2.0 to 3.0	0.683 [0.642, 0.723]	0.135 [0.125, 0.146]
2.5 to 3.5	0.692 [0.632, 0.748]	0.118 [0.111, 0.128]
3.0 to 4.0	0.657 [0.603, 0.709]	0.086 [0.080, 0.092]
3.5 to 4.5	0.623 [0.582, 0.660]	0.111 [0.105, 0.116]
4.0 to 5.0	0.619 [0.582, 0.654]	0.126 [0.118, 0.131]
4.5 to 5.5	0.624 [0.537, 0.711]	0.119 [0.103, 0.135]
5.0 to 6.0	0.639 [0.582, 0.696]	0.121 [0.103, 0.138]

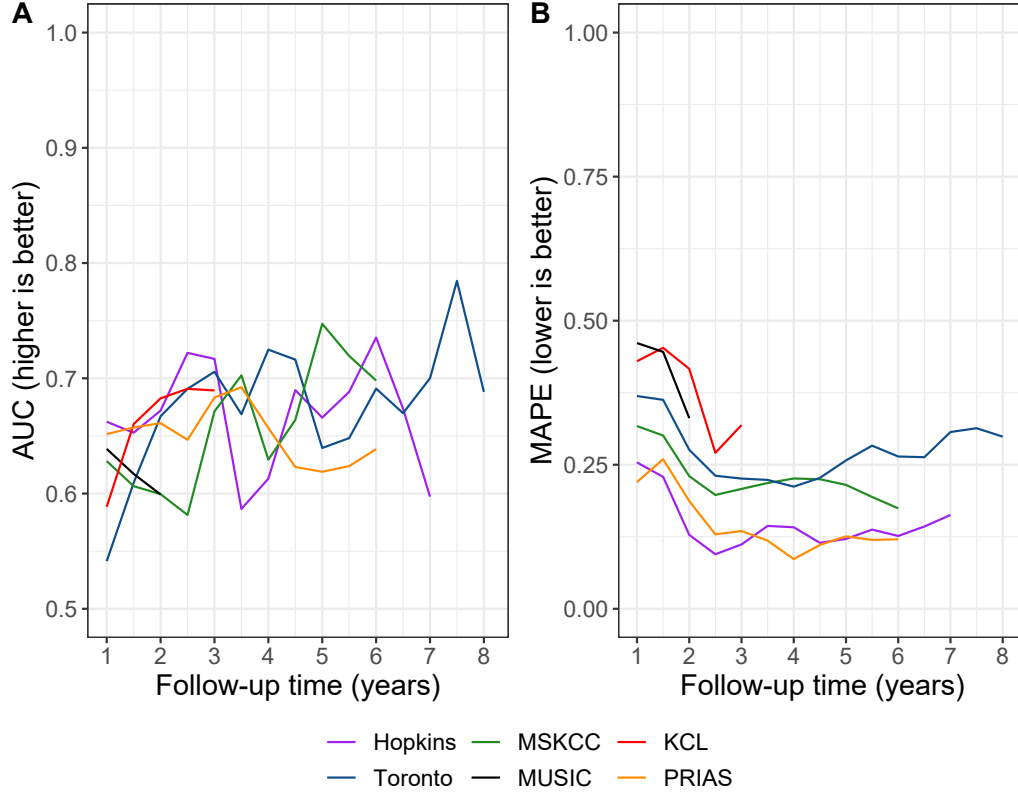


Figure 8: **Validation of dynamic predictions of cause-specific cumulative upgrading-risk.** In **Panel A** we can see that the time dependent area under the receiver operating characteristic curve or AUC (measure of discrimination) is above 0.5 in PRIAS (internal validation), and in Toronto, Hopkins, MSKCC, KCL, and MUSIC AS cohorts (external validation). In **Panel B** we can see that the time dependent root mean squared prediction error or MAPE (measure of calibration) is similar for PRIAS and Hopkins cohorts. The bootstrapped 95% confidence interval for these estimates are presented in Table 8 to Table 12. Full names of Cohorts are *PRIAS*: Prostate Cancer International Active Surveillance, *Toronto*: University of Toronto Active Surveillance, *Hopkins*: Johns Hopkins Active Surveillance, *MSKCC*: Memorial Sloan Kettering Cancer Center Active Surveillance, *KCL*: King's College London Active Surveillance, *MUSIC*: Michigan Urological Surgery Improvement Collaborative Active Surveillance.

Table 9: **External validation of predictions of upgrading in University of Toronto Active Surveillance cohort.** The area under the receiver operating characteristic curve or AUC (measure of discrimination) and mean absolute prediction error or MAPE (measure of calibration) are calculated over the follow-up period at a gap of 6 months. In addition bootstrapped 95% confidence intervals (CI) are also presented.

Follow-up period (years)	AUC (95% CI)	MAPE (95%CI)
0.0 to 1.0	0.541 [0.470, 0.621]	0.369 [0.352, 0.381]
0.5 to 1.5	0.609 [0.547, 0.661]	0.363 [0.348, 0.376]
1.0 to 2.0	0.667 [0.634, 0.712]	0.276 [0.259, 0.296]
1.5 to 2.5	0.691 [0.651, 0.730]	0.231 [0.205, 0.254]
2.0 to 3.0	0.706 [0.637, 0.762]	0.226 [0.196, 0.260]
2.5 to 3.5	0.669 [0.586, 0.741]	0.224 [0.195, 0.258]
3.0 to 4.0	0.725 [0.649, 0.806]	0.212 [0.184, 0.238]
3.5 to 4.5	0.716 [0.642, 0.793]	0.227 [0.206, 0.258]
4.0 to 5.0	0.640 [0.579, 0.717]	0.257 [0.222, 0.312]
4.5 to 5.5	0.648 [0.579, 0.740]	0.283 [0.247, 0.326]
5.0 to 6.0	0.691 [0.608, 0.793]	0.264 [0.232, 0.302]
5.5 to 6.5	0.670 [0.543, 0.776]	0.263 [0.227, 0.307]
6.0 to 7.0	0.700 [0.544, 0.851]	0.307 [0.258, 0.363]
6.5 to 7.5	0.785 [0.640, 0.866]	0.313 [0.272, 0.360]
7.0 to 8.0	0.688 [0.532, 0.786]	0.299 [0.249, 0.361]

Table 10: **External validation of predictions of upgrading in Johns Hopkins Active Surveillance cohort.** The area under the receiver operating characteristic curve or AUC (measure of discrimination) and mean absolute prediction error or MAPE (measure of calibration) are calculated over the follow-up period at a gap of 6 months. In addition bootstrapped 95% confidence intervals (CI) are also presented.

Follow-up period (years)	AUC (95% CI)	MAPE (95%CI)
0.0 to 1.0	0.662 [0.586, 0.715]	0.254 [0.245, 0.265]
0.5 to 1.5	0.653 [0.603, 0.707]	0.229 [0.219, 0.240]
1.0 to 2.0	0.672 [0.604, 0.744]	0.128 [0.115, 0.141]
1.5 to 2.5	0.722 [0.652, 0.792]	0.095 [0.081, 0.111]
2.0 to 3.0	0.717 [0.638, 0.777]	0.112 [0.100, 0.123]
2.5 to 3.5	0.587 [0.493, 0.704]	0.144 [0.129, 0.154]
3.0 to 4.0	0.613 [0.486, 0.742]	0.141 [0.126, 0.156]
3.5 to 4.5	0.690 [0.594, 0.783]	0.115 [0.100, 0.133]
4.0 to 5.0	0.666 [0.572, 0.754]	0.121 [0.104, 0.147]
4.5 to 5.5	0.688 [0.519, 0.779]	0.137 [0.119, 0.161]
5.0 to 6.0	0.735 [0.676, 0.820]	0.126 [0.102, 0.152]
5.5 to 6.5	0.674 [0.581, 0.765]	0.143 [0.121, 0.172]
6.0 to 7.0	0.597 [0.472, 0.712]	0.163 [0.126, 0.195]

Table 11: **External validation of predictions of upgrading in Memorial Sloan Kettering Cancer Center Active Surveillance cohort.** The area under the receiver operating characteristic curve or AUC (measure of discrimination) and mean absolute prediction error or MAPE (measure of calibration) are calculated over the follow-up period at a gap of 6 months. In addition bootstrapped 95% confidence intervals (CI) are also presented.

Follow-up period (years)	AUC (95% CI)	MAPE (95%CI)
0.0 to 1.0	0.628 [0.577, 0.688]	0.317 [0.316, 0.318]
0.5 to 1.5	0.606 [0.532, 0.657]	0.301 [0.290, 0.311]
1.0 to 2.0	0.599 [0.518, 0.671]	0.230 [0.207, 0.256]
1.5 to 2.5	0.581 [0.504, 0.663]	0.198 [0.168, 0.235]
2.0 to 3.0	0.671 [0.599, 0.741]	0.208 [0.182, 0.232]
2.5 to 3.5	0.703 [0.610, 0.777]	0.218 [0.197, 0.246]
3.0 to 4.0	0.629 [0.499, 0.706]	0.226 [0.194, 0.259]
3.5 to 4.5	0.664 [0.589, 0.756]	0.225 [0.199, 0.262]
4.0 to 5.0	0.747 [0.642, 0.841]	0.215 [0.188, 0.247]
4.5 to 5.5	0.719 [0.597, 0.852]	0.194 [0.165, 0.232]
5.0 to 6.0	0.698 [0.565, 0.792]	0.174 [0.136, 0.227]

Table 12: **External validation of predictions of upgrading in King's College London Active Surveillance cohort.** The area under the receiver operating characteristic curve or AUC (measure of discrimination) and mean absolute prediction error or MAPE (measure of calibration) are calculated over the follow-up period at a gap of 6 months. In addition bootstrapped 95% confidence intervals (CI) are also presented.

Follow-up period (years)	AUC (95% CI)	MAPE (95%CI)
0.0 to 1.0	0.589 [0.514, 0.653]	0.430 [0.407, 0.450]
0.5 to 1.5	0.660 [0.550, 0.742]	0.453 [0.431, 0.474]
1.0 to 2.0	0.683 [0.604, 0.753]	0.416 [0.396, 0.445]
1.5 to 2.5	0.691 [0.621, 0.766]	0.271 [0.246, 0.297]
2.0 to 3.0	0.689 [0.616, 0.785]	0.319 [0.282, 0.344]

Table 13: **External validation of predictions of upgrading in Michigan Urological Surgery Improvement Collaborative Active Surveillance cohort.** The area under the receiver operating characteristic curve or AUC (measure of discrimination) and mean absolute prediction error or MAPE (measure of calibration) are calculated over the follow-up period at a gap of 6 months. In addition bootstrapped 95% confidence intervals (CI) are also presented.

Follow-up period (years)	AUC (95% CI)	MAPE (95%CI)
0.0 to 1.0	0.639 [0.607, 0.672]	0.461 [0.450, 0.469]
0.5 to 1.5	0.617 [0.588, 0.652]	0.446 [0.441, 0.453]
1.0 to 2.0	0.599 [0.553, 0.632]	0.331 [0.317, 0.348]

## 160 Appendix C. Personalized Biopsies Based on Cause-Specific Cu- 161 mulative Upgrading-Risk

162 Consider some real patients from the PRIAS database shown in Figure 9–  
163 11. We intend to develop personalized schedule of biopsies for these patients.  
164 Using the joint model fitted to the PRIAS dataset, we first obtain their  
165 cause-specific cumulative upgrading-risk over the entire follow-up period (see  
166 Equation 4), given their accumulated clinical data. Our aim is to employ this  
167 cumulative-risk function in the personalized biopsy schedule. However, in line  
168 with the protocols of most AS cohorts [12], we first schedule a compulsory  
169 biopsy at year one of follow-up. This promises early detection of Gleason  
170 upgrade for patients misdiagnosed as low-grade cancer patients, or patients  
171 who chose AS despite having a higher grade at diagnosis. We also maintain  
172 a recommended minimum gap of one year between consecutive biopsies [11].  
173 Consequently, we schedule personalized biopsies starting from year two until  
174 year a maximum horizon (Table 14). The added benefit of this approach is  
175 that due to the longitudinal measurements accumulated over two years, and  
176 year one biopsy results, we are able to make reasonably accurate predictions  
177 of the cause-specific cumulative upgrading-risk.

We next exploit PRIAS cohort’s fixed schedule of longitudinal measure-  
ments  $L = \{2, 2.5 \dots 6\}$  between year two and six (horizon, Table 14). More  
specifically, we schedule a biopsy at all those future visits where the condi-  
tional cause-specific cumulative upgrading-risk is larger than a certain thresh-  
old  $0 \leq \kappa \leq 1$  (e.g., 10% risk). The resulting personalized schedule of biopsies  
 $B_j^\kappa$  is given by:

$$B_j^\kappa = \left\{ b_{jk} \in L \mid R_j(b_{jk} \mid b_{jk-1}, s) \geq \kappa \wedge (b_{jk} - b_{jk-1} \geq 1) \right\}, \quad (6)$$

178 where  $b_{jk}$  is the time of the  $k$ -th biopsy for the  $j$ -th patient and  $b_{j0}$  cor-  
179 responds to time of the last conducted biopsy before making this sched-  
180 ule. The conditional cause-specific cumulative upgrading-risk denoted by  
181  $R_j(b_{jk} \mid b_{jk-1}, s)$  is defined as in Equation (4). In this risk the contribution  
182 of the observed PSA  $\mathcal{Y}_j(s)$  does not change while scheduling subsequent biop-  
183 sies. However, the ‘conditional’ part here is that successive  $k$ -th biopsy at  
184 time  $b_{jk}$  is scheduled by accounting for the possibility that Gleason upgrade  
185 may not have occurred until the previously scheduled biopsy  $T_j^* > b_{jk-1}$ . The  
186 personalized schedule Equation (6) is updated as more patient data becomes  
187 available over follow-up.



Table 14: **Maximum follow-up period up to which we can reliably make personalized schedules.** In each cohort, this time point is chosen such that there are at least 10 patients who experience upgrading after this time point. Full names of Cohorts are *PRIAS*: Prostate Cancer International Active Surveillance, *Toronto*: University of Toronto Active Surveillance, *Hopkins*: Johns Hopkins Active Surveillance, *MSKCC*: Memorial Sloan Kettering Cancer Center Active Surveillance, *KCL*: King’s College London Active Surveillance, *MUSIC*: Michigan Urological Surgery Improvement Collaborative Active Surveillance.

Cohort	Maximum Personalized Schedule Time (years)
PRIAS	6
KCL	3
MUSIC	2
Toronto	8
MSKCC	6
Hopkins	7

To assist patients in making an informed choice for a schedule, be it personalized or fixed, we provide them patient-specific consequences of following each schedule. To this end, we first calculate the probability of occurrence of upgrading between successive biopsies of each schedule. Using these probabilities we then obtain the expected delay in detection of upgrading for following that schedule. Thus, patients have a method to compare across various schedules in terms of the personalized burden (time and total biopsies), and personalized benefit (less delay in detection of upgrading is beneficial). Suppose once again that for patient  $j$ , the time of latest negative biopsy is  $t$ , and current visit time is  $s > t$ . Then equation for the expected delay  $D_j(B | t, s)$  in detection of upgrading using schedule of biopsies  $B = \{b_1, \dots, b_h\}$ , where  $b_1 \geq s$ , and  $b_h$  is the horizon time (Table 14) up to which we want to schedule biopsies, is given by:

$$D_j(B | t, s) = \sum_{v=1}^h R_j(b_v | b_{v-1}, s) \times \left\{ b_v - b_{v-1} - \int_{b_{v-1}}^{b_v} S_j(u | b_v, b_{v-1}, s) du \right\},$$

$$S_j(u | b_v, b_{v-1}, s) = \Pr\{T_j^* > u | b_v \geq T_j^* > b_{v-1}, \mathcal{Y}_j(s), \mathcal{D}_n\}, \quad b_v \geq u > b_{v-1}, \quad (7)$$

188 and  $R_j(b_v | b_{v-1}, s)$  is as defined in Equation (4). The personalized and fixed  
189 schedules, and their consequences for a few real patients from the PRIAS  
190 dataset are shown in Figure 9 to Figure 11. A compulsory biopsy was done

191 at horizon  $b_h$  of follow-up in all schedules for meaningful comparison of their  
192 expected delays in detection of upgrading.

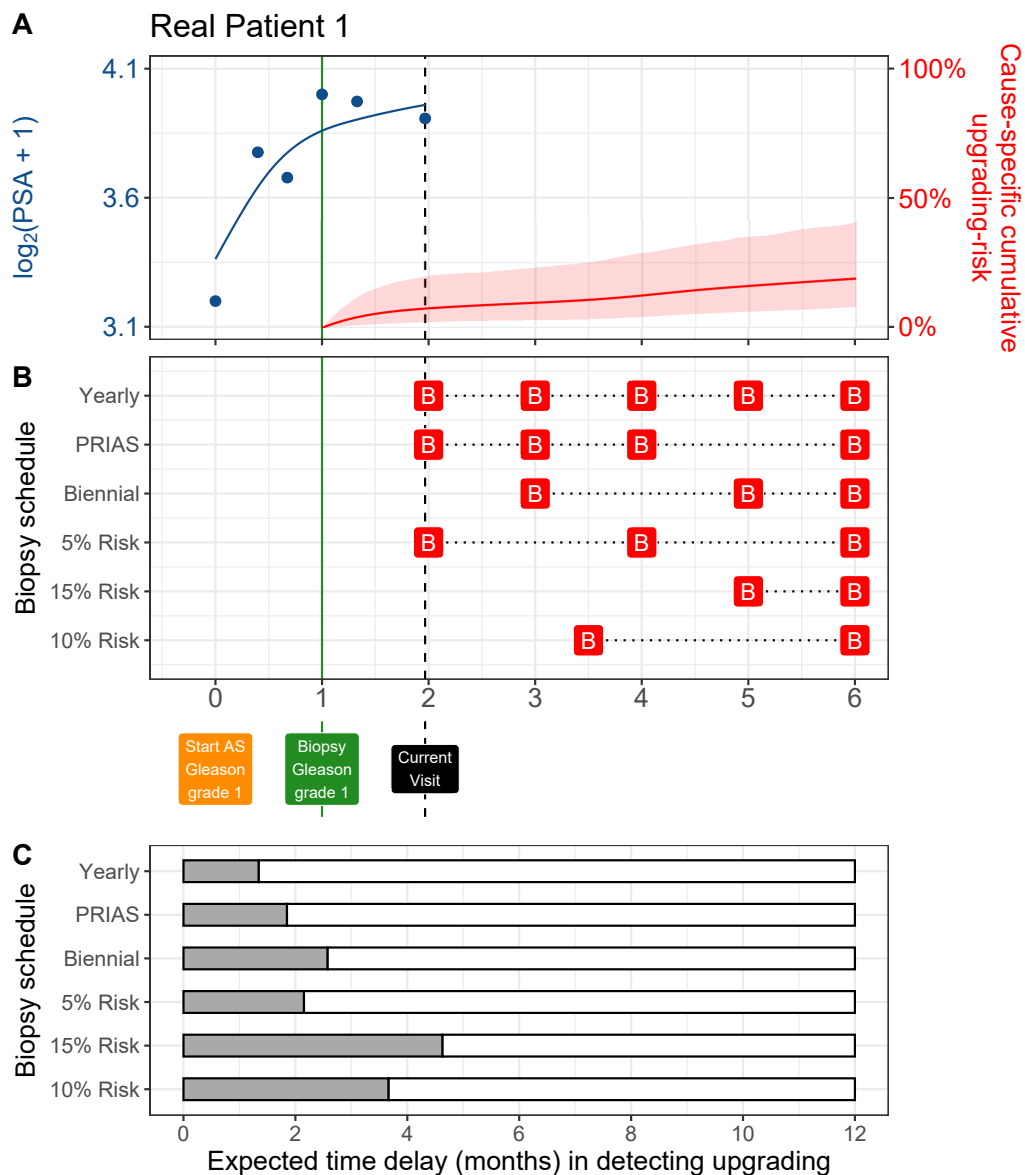


Figure 9: **Personalized and fixed schedules of biopsies for patient 1.** **Panel A:** shows the observed and fitted  $\log_2(\text{PSA} + 1)$  measurements (Equation 1), and the dynamic cause-specific cumulative upgrading-risk (see Appendix B) over follow-up period. **Panel B** shows the personalized and fixed schedules of biopsies with a 'B' indicating times of biopsies. **Panel C** compares various schedules in terms of the expected delay in detection of upgrading if they are followed. A compulsory biopsy was scheduled at year six (maximum biopsy scheduling time in PRIAS, Supplementary C) in all schedules for a meaningful comparison between them.

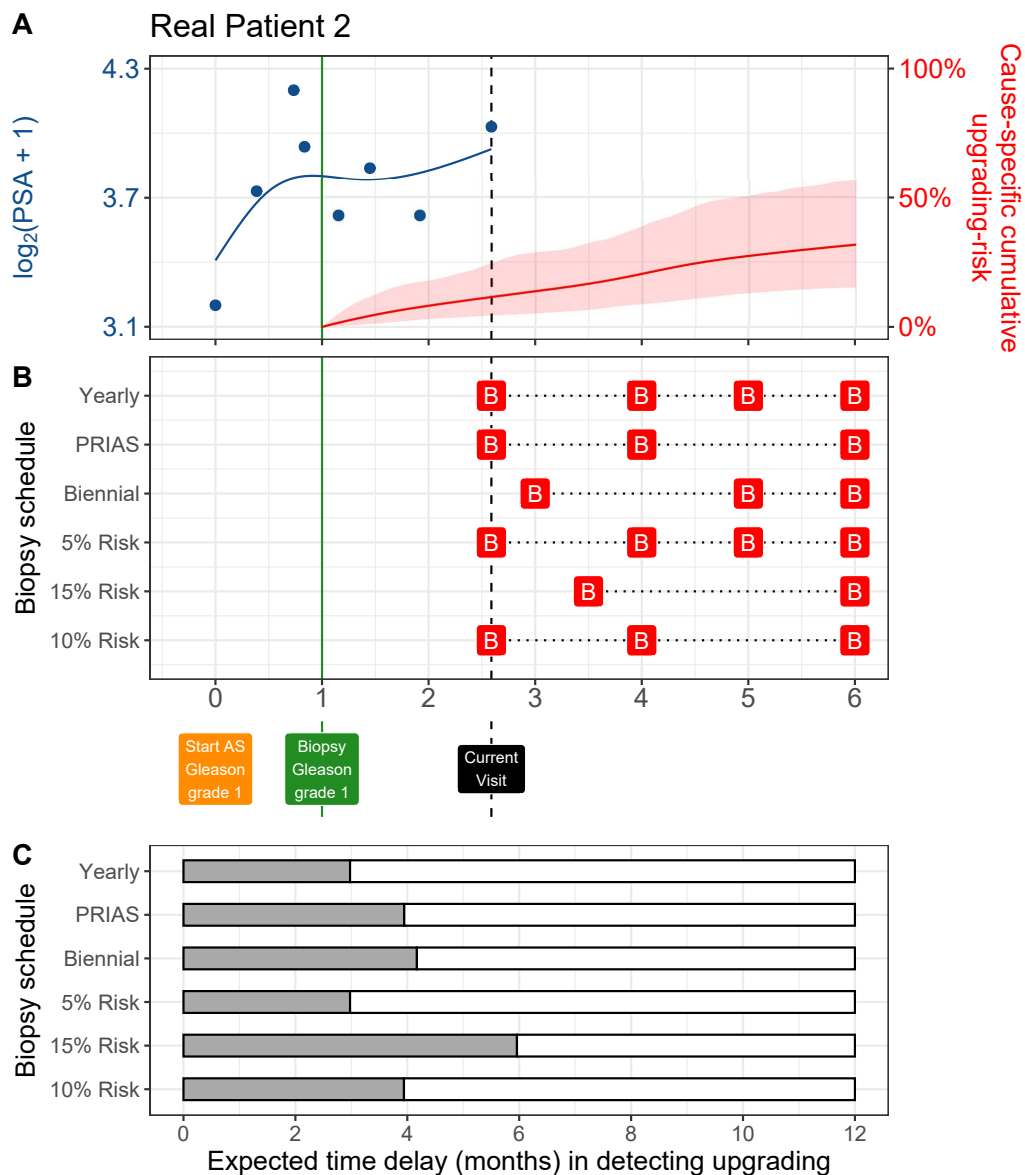


Figure 10: **Personalized and fixed schedules of biopsies for patient 2.** **Panel A:** shows the observed and fitted  $\log_2(\text{PSA} + 1)$  measurements (Equation 1), and the dynamic cause-specific cumulative upgrading-risk (see Appendix B) over follow-up period. **Panel B** shows the personalized and fixed schedules of biopsies with a 'B' indicating times of biopsies. **Panel C** compares various schedules in terms of the expected delay in detection of upgrading if they are followed. A compulsory biopsy was scheduled at year six (maximum biopsy scheduling time in PRIAS, Supplementary C) in all schedules for a meaningful comparison between them.

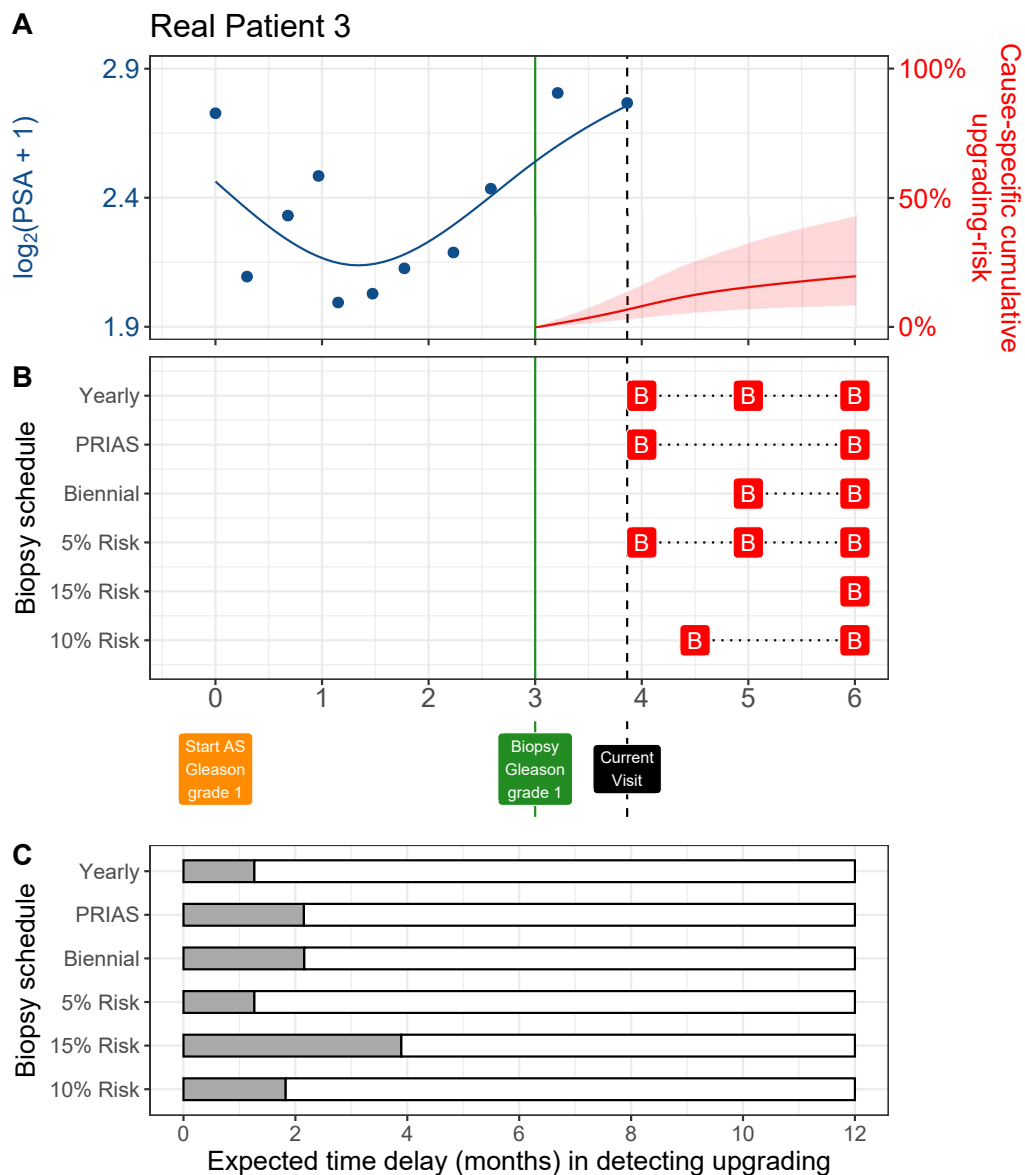


Figure 11: **Personalized and fixed schedules of biopsies for patient 3.** **Panel A:** shows the observed and fitted  $\log_2(\text{PSA} + 1)$  measurements (Equation 1), and the dynamic cause-specific cumulative upgrading-risk (see Appendix B) over follow-up period. **Panel B** shows the personalized and fixed schedules of biopsies with a 'B' indicating times of biopsies. **Panel C** compares various schedules in terms of the expected delay in detection of upgrading if they are followed. A compulsory biopsy was scheduled at year six (maximum biopsy scheduling time in PRIAS, Supplementary C) in all schedules for a meaningful comparison between them.

## Appendix D. Web Application for Practical Use of Personalized Schedule of Biopsies

We implemented our methodology in a web-application to assist patients and doctors in better decision making. It works on desktop as well as mobile devices. The cohorts that are currently supported in this web-application are PRIAS and the largest five cohorts from the GAP3 database [6]. These are the University of Toronto AS (Toronto), Johns Hopkins AS (Hopkins), Memorial Sloan Kettering Cancer Center AS (MSKCC), King's College London AS (KCL), and Michigan Urological Surgery Improvement Collaborative AS (MUSIC). The web-application is hosted at [https://emcbiostatistics.shinyapps.io/prias\\_biopsy\\_recommender/](https://emcbiostatistics.shinyapps.io/prias_biopsy_recommender/).

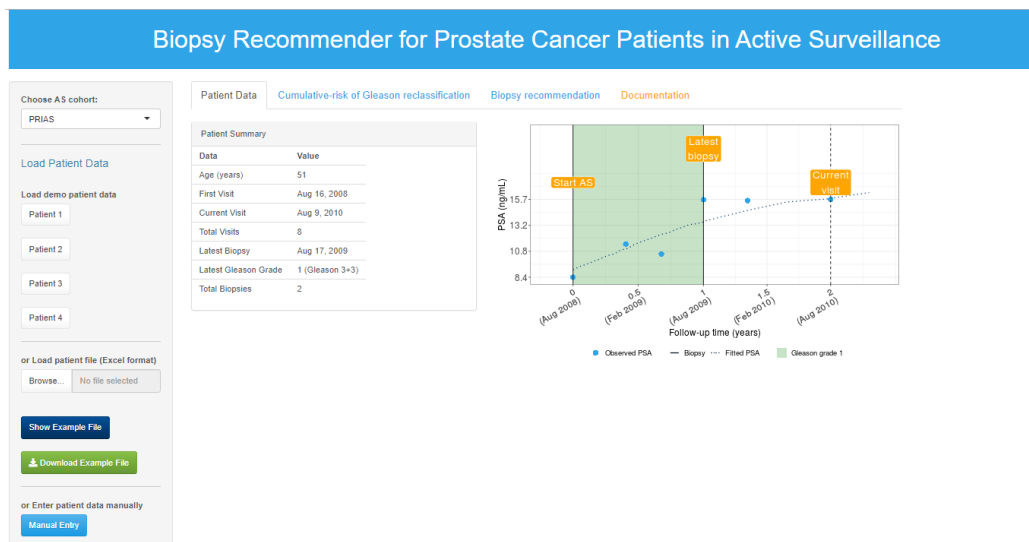


Figure 12: Landing page of the web-application. Panel on the left allows users to load patient data and panel on the right provides information. Patient data can be entered manually, or via Excel files. In addition, demo patient data is already uploaded to assist users in understanding the web-application.

## 204 Appendix E. Source Code

205 The R code for fitting the joint model to the PRIAS dataset, is at [https:](https://github.com/anirudhtomer/prias/tree/master/src/clinical_gap3)  
 206 [//github.com/anirudhtomer/prias/tree/master/src/clinical\\_gap3](https://github.com/anirudhtomer/prias/tree/master/src/clinical_gap3). We  
 207 refer to this location as ‘R\_HOME’ in the rest of this document.

### 208 *Appendix E.1. Fitting the Joint Model to the PRIAS dataset*

209 **Accessing the dataset:** The PRIAS dataset is not openly accessible.  
 210 However, access to the database can be requested via the contact links at  
 211 <https://www.prias-project.org>.

212  
 213 **Formatting the dataset:** This dataset however is in the so-called wide  
 214 format and also requires removal of incorrect entries. This can be done  
 215 via the R script `R_HOME/dataset_cleaning.R`. This will lead to two R  
 216 objects, namely ‘`prias_final.id`’ and ‘`prias_long_final`’. The ‘`prias_final.id`’ ob-  
 217 ject contains information about time of upgrading for PRIAS patients. The  
 218 ‘`prias_long_final`’ object contains longitudinal PSA measurements, the time  
 219 of biopsies and results of biopsies.

220  
 221 **Fitting the joint model:** We use a joint model for time to event and  
 222 longitudinal data to model the evolution of PSA measurements over time,  
 223 and to simultaneously model their association with the risk of upgrading.  
 224 The R package we use for this purpose is called **JMbayes** ([https://cran.r-](https://cran.r-project.org/web/packages/JMbayes/JMbayes.pdf)  
 225 [project.org/web/packages/JMbayes/JMbayes.pdf](https://cran.r-project.org/web/packages/JMbayes/JMbayes.pdf)). The API we use, how-  
 226 ever, are currently not hosted on CRAN, and can be found here: [https:](https://github.com/anirudhtomer/JMbayes)  
 227 [//github.com/anirudhtomer/JMbayes](https://github.com/anirudhtomer/JMbayes). The joint model can be fitted via  
 228 the script `R_HOME/analysis.R`. It takes roughly 6 hours to run on an Intel  
 229 core-i5 machine with 4 cores, and 8GB of RAM.

230 The graphs presented in the main manuscript, and the supplementary  
 231 material can be generated by the scripts in `R_HOME/plots/`.

### 232 *Appendix E.2. Validation of Predictions of Upgrading*

233 Validations can be done using the scripts `R_HOME/validation/auc_brier/`  
 234 `auc_calculator.R`, and `R_HOME/validation/auc_brier/gof_calculator.`  
 235 `R`. For external validation access to GAP3 database is required.

236 *Appendix E.3. Creating Personalized Schedules of Biopsies*

237     Once a joint model is fitted to the PRIAS dataset, personalized schedules  
238 of biopsies based on risk of upgrading for new patients can be developed us-  
239 ing the script `R_HOME/scheduleCreator.R`. This script also provides fixed  
240 biopsy schedules for the patients. In addition with each schedule, the ex-  
241 pected delay in detection of upgrading is also provided.

242 *Appendix E.4. Source Code for Web Application*

243     Source for the shiny web application which provides biopsy schedules for  
244 patients can be found at `R_HOME/shinyapp`



245 **Appendix F. Appendix A. Members of The Movember Founda-**  
 246 **tions Global Action Plan Prostate Cancer Active Surveil-**  
 247 **lance (GAP3) consortium**

248 *Principle Investigators:* Bruce Trock (Johns Hopkins University, The  
 249 James Buchanan Brady Urological Institute, Baltimore, USA), Behfar Ehdaie  
 250 (Memorial Sloan Kettering Cancer Center, New York, USA), Peter Car-  
 251 roll (University of California San Francisco, San Francisco, USA), Christo-  
 252 pher Filson (Emory University School of Medicine, Winship Cancer Insti-  
 253 tute, Atlanta, USA), Jeri Kim / Christopher Logothetis (MD Anderson  
 254 Cancer Centre, Houston, USA), Todd Morgan (University of Michigan and  
 255 Michigan Urological Surgery Improvement Collaborative (MUSIC), Michi-  
 256 gan, USA), Laurence Klotz (University of Toronto, Sunnybrook Health Sci-  
 257 ences Centre, Toronto, Ontario, Canada), Tom Pickles (University of British  
 258 Columbia, BC Cancer Agency, Vancouver, Canada), Eric Hyndman (Uni-  
 259 versity of Calgary, Southern Alberta Institute of Urology, Calgary, Canada),  
 260 Caroline Moore (University College London & University College London  
 261 Hospital Trust, London, UK), Vincent Gnanapragasam (University of Cam-  
 262 bridge & Cambridge University Hospitals NHS Foundation Trust, Cam-  
 263 bridge, UK), Mieke Van Hemelrijck (King's College London, London, UK  
 264 & Guys and St Thomas NHS Foundation Trust, London, UK), Prokar Das-  
 265 gupta (Guys and St Thomas NHS Foundation Trust, London, UK), Chris  
 266 Bangma (Erasmus Medical Center, Rotterdam, The Netherlands/ represen-  
 267 tative of Prostate cancer Research International Active Surveillance (PRIAS)  
 268 consortium), Monique Roobol (Erasmus Medical Center, Rotterdam, The  
 269 Netherlands/ representative of Prostate cancer Research International Active  
 270 Surveillance (PRIAS) consortium), Arnauld Villers (Lille University Hospi-  
 271 tal Center, Lille, France), Antti Rannikko (Helsinki University and Helsinki  
 272 University Hospital, Helsinki, Finland), Riccardo Valdagni (Department of  
 273 Oncology and Hemato-oncology, Universit degli Studi di Milano, Radia-  
 274 tion Oncology 1 and Prostate Cancer Program, Fondazione IRCCS Istituto  
 275 Nazionale dei Tumori, Milan, Italy), Antoinette Perry (University College  
 276 Dublin, Dublin, Ireland), Jonas Hugosson (Sahlgrenska University Hospital,  
 277 Gteborg, Sweden), Jose Rubio-Briones (Instituto Valenciano de Oncologa,  
 278 Valencia, Spain), Anders Bjartell (Skne University Hospital, Malm, Swe-  
 279 den), Lukas Hefermehl (Kantonsspital Baden, Baden, Switzerland), Lee Lui  
 280 Shiong (Singapore General Hospital, Singapore, Singapore), Mark Fryden-  
 281 berg (Monash Health; Monash University, Melbourne, Australia), Yoshiyuki

282 Kakehi / Mikio Sugimoto (Kagawa University Faculty of Medicine, Kagawa,  
 283 Japan), Byung Ha Chung (Gangnam Severance Hospital, Yonsei University  
 284 Health System, Seoul, Republic of Korea)

285 *Pathologist:* Theo van der Kwast (Princess Margaret Cancer Centre,  
 286 Toronto, Canada). Technology Research Partners: Henk Obbink (Royal  
 287 Philips, Eindhoven, the Netherlands), Wim van der Linden (Royal Philips,  
 288 Eindhoven, the Netherlands), Tim Hulsen (Royal Philips, Eindhoven, the  
 289 Netherlands), Cees de Jonge (Royal Philips, Eindhoven, the Netherlands).

290 *Advisory Regional statisticians:* Mike Kattan (Cleveland Clinic, Cleve-  
 291 land, Ohio, USA), Ji Xinge (Cleveland Clinic, Cleveland, Ohio, USA), Ken-  
 292 neth Muir (University of Manchester, Manchester, UK), Artitaya Lophatananon  
 293 (University of Manchester, Manchester, UK), Michael Fahey (Epworth Health-  
 294 Care, Melbourne, Australia), Ewout Steyerberg (Erasmus Medical Center,  
 295 Rotterdam, The Netherlands), Daan Nieboer (Erasmus Medical Center, Rot-  
 296 terdam, The Netherlands); Liying Zhang (University of Toronto, Sunnybrook  
 297 Health Sciences Centre, Toronto, Ontario, Canada)

298 *Executive Regional statisticians:* Ewout Steyerberg (Erasmus Medical  
 299 Center, Rotterdam, The Netherlands), Daan Nieboer (Erasmus Medical Cen-  
 300 ter, Rotterdam, The Netherlands); Kerri Beckmann (King's College London,  
 301 London, UK & Guys and St Thomas NHS Foundation Trust, London, UK),  
 302 Brian Denton (University of Michigan, Michigan, USA), Andrew Hayen (Uni-  
 303 versity of Technology Sydney, Australia), Paul Boutros (Ontario Institute of  
 304 Cancer Research, Toronto, Ontario, Canada).

305 *Clinical Research Partners IT Experts:* Wei Guo (Johns Hopkins Uni-  
 306 versity, The James Buchanan Brady Urological Institute, Baltimore, USA),  
 307 Nicole Benfante (Memorial Sloan Kettering Cancer Center, New York, USA),  
 308 Janet Cowan (University of California San Francisco, San Francisco, USA),  
 309 Dattatraya Patil (Emory University School of Medicine, Winship Cancer In-  
 310 stitute, Atlanta, USA), Emily Tolosa (MD Anderson Cancer Centre, Hous-  
 311 ton, Texas, USA), Tae-Kyung Kim (University of Michigan and Michigan  
 312 Urological Surgery Improvement Collaborative, Ann Arbor, Michigan, USA),  
 313 Alexandre Mamedov (University of Toronto, Sunnybrook Health Sciences  
 314 Centre, Toronto, Ontario, Canada), Vincent LaPointe (University of British  
 315 Columbia, BC Cancer Agency, Vancouver, Canada), Trafford Crump (Uni-  
 316 versity of Calgary, Southern Alberta Institute of Urology, Calgary, Canada),  
 317 Vasilis Stavrinides (University College London & University College Lon-  
 318 don Hospital Trust, London, UK), Jenna Kimberly-Duffell (University of  
 319 Cambridge & Cambridge University Hospitals NHS Foundation Trust, Cam-

bridge, UK), Aida Santaolalla (King's College London, London, UK & Guys  
and St Thomas NHS Foundation Trust, London, UK), Daan Nieboer (Eras-  
mus Medical Center, Rotterdam, The Netherlands), Jonathan Olivier (Lille  
University Hospital Center, Lille, France), Tiziana Rancati (Fondazione IR-  
CCS Istituto Nazionale dei Tumori di Milano, Milan, Italy), Heln Ahlgren  
(Sahlgrenska University Hospital, Gteborg, Sweden), Juanma Mascars (Insti-  
tuto Valenciano de Oncologa, Valencia, Spain), Annica Lfgren (Skne Univer-  
sity Hospital, Malm, Sweden), Kurt Lehmann (Kantonsspital Baden, Baden,  
Switzerland), Catherine Han Lin (Monash University and Epworth Health-  
Care, Melbourne, Australia), Hiromi Hiram (Kagawa University, Kagawa,  
Japan), Kwang Suk Lee (Yonsei University College of Medicine, Gangnam  
Severance Hospital, Seoul, Korea).

*Research Advisory Committee:* Guido Jenster (Erasmus MC, Rotterdam,  
the Netherlands), Anssi Auvinen (University of Tampere, Tampere, Finland),  
Anders Bjartell (Skne University Hospital, Malm, Sweden), Masoom Haider  
(University of Toronto, Toronto, Canada), Kees van Bochove (The Hyve  
B.V. Utrecht, Utrecht, the Netherlands), Ballentine Carter (Johns Hopkins  
University, Baltimore, USA until 2018).

*Management team:* Sam Gledhill (Movember Foundation, Melbourne,  
Australia), Mark Buzza / Michelle Kouspou (Movember Foundation, Mel-  
bourne, Australia), Chris Bangma (Erasmus Medical Center, Rotterdam,  
The Netherlands), Monique Roobol (Erasmus Medical Center, Rotterdam,  
The Netherlands), Sophie Bruinsma / Jozien Helleman (Erasmus Medical  
Center, Rotterdam, The Netherlands).

## References

1. Epstein JI, Egevad L, Amin MB, Delahunt B, Srigley JR, Humphrey PA.  
The 2014 international society of urological pathology (isup) consensus  
conference on gleason grading of prostatic carcinoma. *The American  
journal of surgical pathology* 2016;40(2):244–52.
2. Pearson JD, Morrell CH, Landis PK, Carter HB, Brant LJ. Mixed-  
effects regression models for studying the natural history of prostate  
disease. *Statistics in Medicine* 1994;13(5-7):587–601.
3. Lin H, McCulloch CE, Turnbull BW, Slate EH, Clark LC. A latent  
class mixed model for analysing biomarker trajectories with irregularly  
scheduled observations. *Statistics in Medicine* 2000;19(10):1303–18.

- 355 4. De Boor C. A practical guide to splines; vol. 27. Springer-Verlag New  
356 York; 1978.
- 357 5. Eilers PH, Marx BD. Flexible smoothing with B-splines and penalties.  
358 *Statistical Science* 1996;11(2):89–121.
- 359 6. Bruinsma SM, Zhang L, Roobol MJ, Bangma CH, Steyerberg EW,  
360 Nieboer D, Van Hemelrijck M, consortium MFGAPPCASG, Trock B,  
361 Ehdaie B, et al. The movember foundation’s gap3 cohort: a profile of  
362 the largest global prostate cancer active surveillance database to date.  
363 *BJU international* 2018;121(5):737–44.
- 364 7. Turnbull BW. The empirical distribution function with arbitrarily  
365 grouped, censored and truncated data. *Journal of the Royal Statisti-*  
366 *cal Society Series B (Methodological)* 1976;38(3):290–5.
- 367 8. Rizopoulos D. The R package JMbayes for fitting joint models for lon-  
368 gitudinal and time-to-event data using MCMC. *Journal of Statistical*  
369 *Software* 2016;72(7):1–46.
- 370 9. Rizopoulos D, Molenberghs G, Lesaffre EM. Dynamic predictions with  
371 time-dependent covariates in survival analysis using joint modeling and  
372 landmarking. *Biometrical Journal* 2017;59(6):1261–76.
- 373 10. Steyerberg EW, Vickers AJ, Cook NR, Gerds T, Gonen M, Obuchowski  
374 N, Pencina MJ, Kattan MW. Assessing the performance of prediction  
375 models: a framework for some traditional and novel measures. *Epidemi-*  
376 *ology (Cambridge, Mass)* 2010;21(1):128.
- 377 11. Bokhorst LP, Alberts AR, Rannikko A, Valdagni R, Pickles T, Kakehi Y,  
378 Bangma CH, Roobol MJ, PRIAS study group . Compliance rates with  
379 the Prostate Cancer Research International Active Surveillance (PRIAS)  
380 protocol and disease reclassification in noncompliers. *European Urology*  
381 2015;68(5):814–21.
- 382 12. Nieboer D, Tomer A, Rizopoulos D, Roobol MJ, Steyerberg EW. Active  
383 surveillance: a review of risk-based, dynamic monitoring. *Translational*  
384 *andrology and urology* 2018;7(1):106–15.